Preparation and properties of metallopolymer nanostructures relevant to renewable energy applications

SUMMARY

The fundamental requirement for developing next-generation energy devices is to incorporate precise bonding interactions into the materials to manage the properties of the synthesized materials. Metal-containing polymers are also known as metallopolymers or polymeric composite materials in more recent years [1-3]. The accumulation of state and the charge transport features of the devices are influenced by the molecular structure and the electronic properties of the metallopolymer [4]. Renewable energy sources are used to power flexible energy devices, which have gained a lot of interest as a useful material platform and the diverse fields, which required power to be operated [5]. These materials are created by conjugating inorganic substances that are naturally occurring on Earth with polymeric ligands. By estimating the integration of metal ions or metal complexes in the polymeric chain, we might increase the conductivity of these metal-organic framework systems [6, 7]. Apart from that, orbital linker matching problems make metallopolymers rarely conductible. Contrary to carbon, transition metals can vary their coordination number or oxidation state, and when they are included in polymer chains, they cause a switch between high and low conductivity of material states [8, 9]. Metal-containing polymers, also known as metallopolymers, have gotten a lot of interest in the last few years as a new functional materials platform [10]. Their optoelectronic and catalytic capabilities were just recently discovered. Due to significant developments in surface-initiated or grafting-to procedures, these materials can be used in bulk or to immobilize polymers onto different surfaces, enabling a wide range of surface-decorated and immobilized metallopolymer materials [11].

Renewable energy is energy produced from naturally occurring resources such as the sun, wind, water, and heat from the ground as presented in Fig. 2. These resources are continuously being replaced and will never run out because they are regenerated organically. A clean, sustainable energy source, renewable energy can be utilized to provide heat, electricity, fuel for vehicles, and other energy needs. By employing two or more inorganic component materials, a mixture of conjugated polymers and inorganic materials, or a bulk heterojunction device at the nanoscale to combine an electron-receiving component and an electron-producing component [12, 13]. To attain high currents and fill factors in PV devices, the mobilities of electrons and holes must be adjusted and balanced. This can be helped by enhanced electron transport via the inorganic part of the conjugated polymer [14]. While PEDOT: PSS can be used as an active interlayer to improve device performance, the low absorbance issue can be solved by incorporating an active layer with a high absorbance throughout the entire solar light spectrum into the photoactive layers [15]. In these devices, a large number of donor/acceptor interfaces effectively split photo-generated excitons within their diffusion length, and the liberated charges subsequently travel through bi-continuous interpenetrating transport channels to the corresponding electrodes [16]. Due to the large donor-acceptor interfacial area and direct carrier transport routes, the photovoltaic efficiencies of these devices are greatly influenced by the geometry of the composite structure in contrast to devices with layered structures. High efficiency is usually constrained by poorly organized donor-acceptor interfaces and discontinuous electron transport paths in the active layers [17]. Light absorption, exciton diffusion, and energy transfer towards the heterojunctions are the key processes in the use of metallopolymeric photovoltaic nanomaterials to transform solar energy into electrical energy [18]. Due to the recent use of metallopolymeric and polymeric composite functional materials in molecular electronics, which provides environmentally friendly alternatives to inorganic nanomaterials in a variety of applications, these materials have many extraordinary characteristics, including small size, good abundance, diversity of applications, ease of production, manufacture, and extraordinary performance [19, 20].

In the field of optoelectronics, metallopolymers have interesting uses, specifically as harvesting systems and light-emitting diodes, respectively and many other properties of metallopolymer materials [21]. The structural class benefits while minimizing some of its drawbacks by combining organic ligands with a variety of coordinating metal ions and incorporating them into a polymeric matrix [22]. As a result, materials that are insulating, semiconducting, or even conducting can be produced. Applications in the field of optoelectronics, including photovoltaics, sensors, non-linear optics, and photoswitches, are made possible by the photophysical, electrochemical, and photochemical features of the metal-ligand coordination and its relatively strong interaction [22-24]. The study of metallopolymers has been hampered for a long time by preparation challenges, including difficult characterization problems and difficulties with synthesis and purifying processes. In the presence of metal centers, several of the polymerization methods that are so effective for pure organic monomers were shown to be ineffective or to cause unfavourable side reactions. These methods usually produced intractable materials, tainted with structural flaws, or lacked strong characterizations, as well as low-molar-mass metallopolymers [25]. The advantages of organic/polymer optoelectronic devices, including their flexibility, low cost, and straightforward fabrication procedures, have sped up their development in recent years. Even more intriguing is the fact that metallopolymeric semiconductors permit direct optical transition, making them strong contenders for light-sensitive applications like solar cells and photodetectors. There is currently a great deal of interest in developing renewable energy sources, such as solar energy, as a result of the knowledge that oil supplies of the Earth have a finite lifespan. Therefore, finding novel, highly effective polymeric materials that can be used in solar systems at a reasonable cost is a significant task [25]. π-conjugated organic polymers, such as poly(3hexylthiophene), which have historically suited this role under their comparatively modest bandgaps, are the macromolecular materials most frequently used in these applications [26]. The bandgap affects the solar spectrum that the active layer can absorb and, consequently, the intrinsic efficiency of the device [25, 26]. Due to their limited ionization potential and customizable electronic structural properties, metallopolymers and polymeric composites are ideal for use in ink-jet printing and spin coating on large surfaces [27]. Excitons are produced and the HOMO-LUMO gap is narrowed when these devices are in direct contact with any illumination source. In metallopolymeric systems, electron transport is reliant on the transfer through ligand [28]. Excitons are dissociated in the second step, and they are then gathered at the electrodes in the final procedure [29].

Chapter 1 deals with the fundamental concept behind the metallopolymeric functional nanomaterials because of their exclusive properties, commercial, biodegradability, high elasticity and efficient nature for their various applications in different fields. This chapter contains the recent accomplishments of the ongoing challenges for the metallopolymeric functional materials for their advanced solar energy applications which can affect human life. These materials are useful for the fabrication of economical energy conversion and optoelectronic devices. The domain of the applicability of these materials is very large such as energy devices, sensors/ actuators, biomedical applications, photodetectors and micromechanical devices. Energy conversion devices like photovoltaic solar cells, photodetectors, and light-dependent resistors, triboelectric energy harvesting devices can be manufactured with metallopolymer nanomaterials. When polymers are conjugated with metals, they offer advanced functional opportunities for the advancement of various energy-harvesting materials with their enhanced properties. At the electrodes and photo-detecting material interface, electrostatic induction causes a Helmholtz double layer for achieving equilibrium, with the metal electrodes being negatively charged and the photoactive being positively charged. The internal electric field is induced by the depletion layer, which has an excessively positive charge. In the meantime, as seen in Fig. 1, the electric field causes the photoactive energy bands of the material to bend upward at the contact. The degree of bending of the energy band is equal to the work function difference between the photodetector material and the metal electrodes. The barrier is controlled by the interface states and adsorption, except for the difference in work function. The cause of the grain boundary barrier has been hypothesized to be adsorbed O^{2-} ions. Since these adsorbates are released from the grain border, it is fair to assume that light irradiation lowers the grain boundary barrier. While the holes in the valance band tend to flow toward the metal side, closer to the interface, the generated electrons in the conduction band prefer to move away from the contact. MSM barriers have the same ability to separate and collect the photo-generated electrons and holes because of their identical size, which causes them to cancel each other out in the external circuit in the absence of an external power source. MSM barriers are formed at the interface of the drain and source. Thus, symmetric barrier-based MSM devices always need an external power supply to carry out the operation.

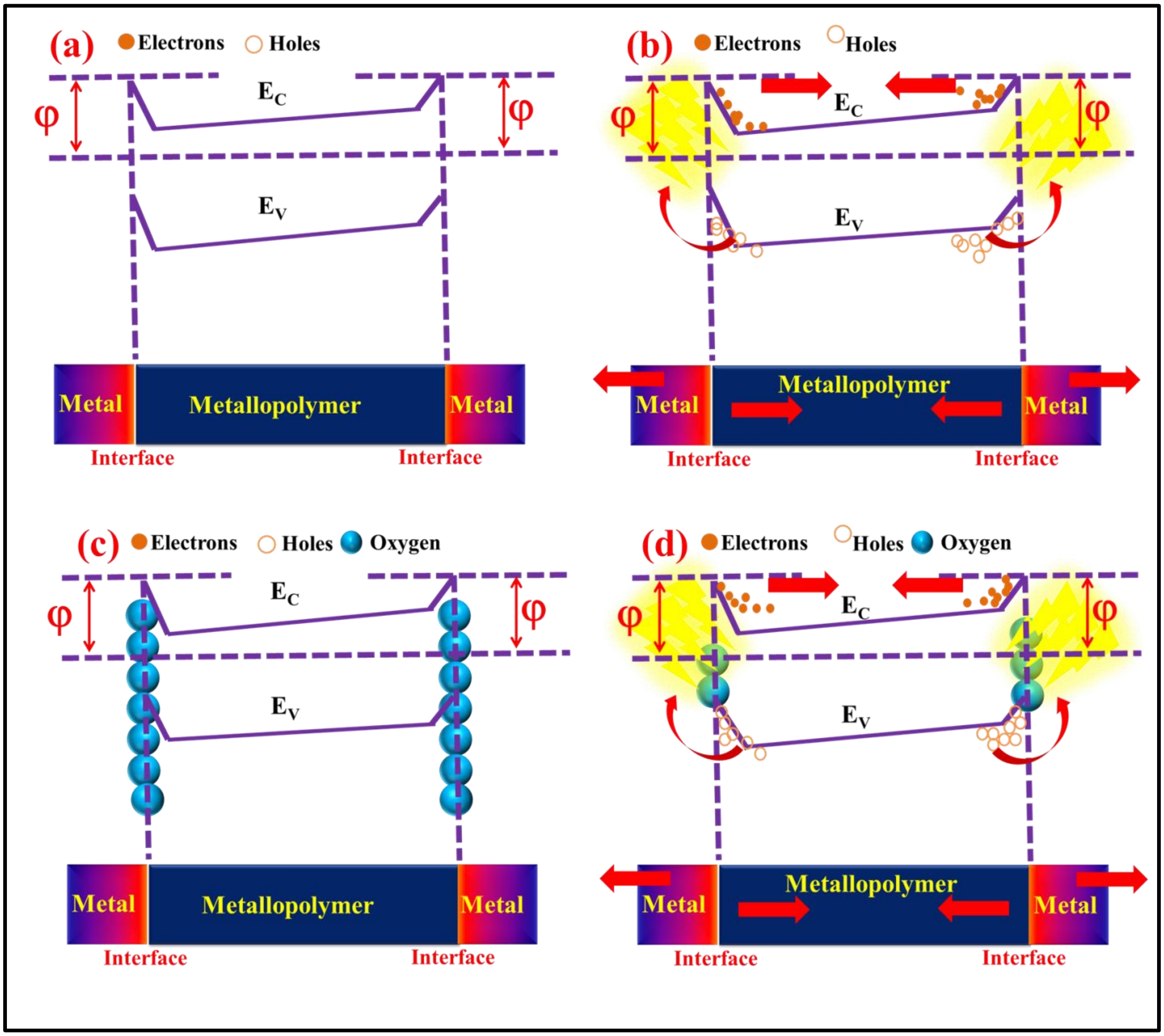

Fig. 1. (a) Band diagram under dark in vacuum condition (b) Band diagram under illumination in vacuum condition (c) Band diagram under dark in ambient atmospheric condition (d) Band diagram under illumination in ambient atmospheric condition.

Chapter 2 reports the solvent-free frontal polymerization of acrylamide monomer with transitional metal dichalcogenide (TMDs) i.e. MoS_2 nanoflakes. Scanning electron microscopy (SEM) images confirm the formation of nanoflakes of MoS_2 and the interface between nanoflakes and polyacrylamide. In this research, we have described the solvent-free frontal polymerization of acrylamide monomer with transition metal dichalcogenide MoS_2, which improves the electrical and charge transport capabilities of polyacrylamide. Metallopolymeric nanostructures are incredibly useful in a wide range of technological fields, particularly as cutting-edge functional materials. As a result, adding MoS_2 nanoflakes to polyacrylamide greatly increases the physical range of limitation beyond that of the host polymer and enables the capabilities of material for clear-cut applications. The band structure was observed from the Raman spectra, which show the E^1_{2g} peak at 384.80 cm^{-1} and 410.03 cm^{-1} respectively in MoS_2-Polyacrylamide. The X-ray diffraction (XRD) pattern revealed the crystallinity of as prepared metallopolymer and Fourier-transform infrared (FTIR**)** spectroscopy confirmed the presence of a surface functional group attached to the metallopolymer. UV-Visible spectra of the metallopolymer nanomaterial exhibited the broad range absorption of the spectrum by metallopolymer. Thermal properties of functionalized metallopolymer were investigated using Thermogravimetric (TG) - Differential thermal analysis (DTA) analysis. Current-voltage (I-V) and time-dependent photoresponse characteristics of MoS_2-Polyacrylamide were carried out under constant exposure to UV light and I-V characteristics and transient photoresponse of the materials are presented in Fig. 2. As prepared metallopolymeric nanomaterial showed enhanced photoconversion performance under ambient conditions. Responsivity and detectivity were found at 60.09 mA/W and 4.96×10^{11} Jones. Rise and decay times were observed as 0.77 s and 0.38 s with the LDR of 60.09 dB at a very low power of 40 $\mu W/ cm^2$.

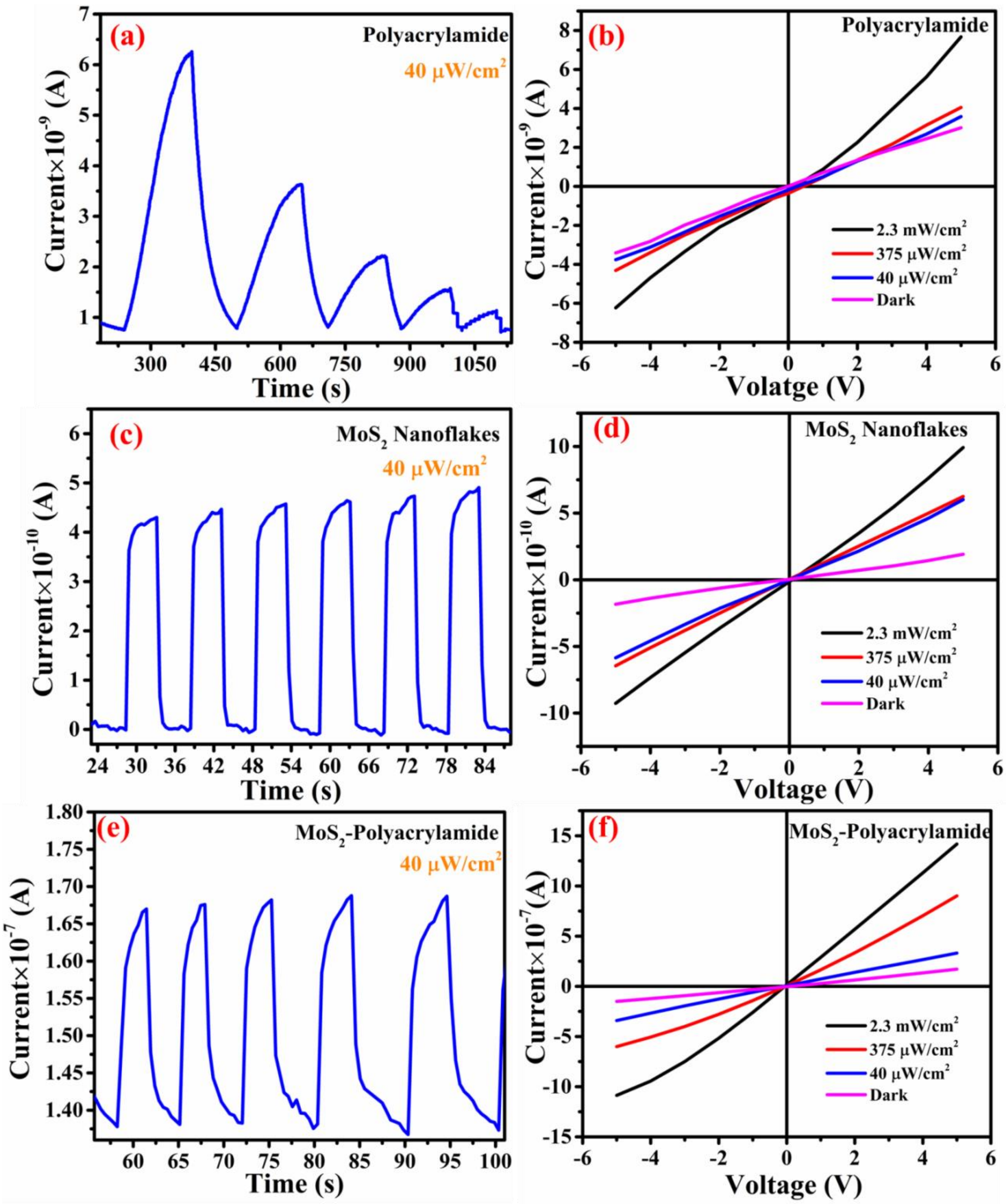

Fig. 2. (a) Time-dependent photoresponse of polyacrylamide (b) I-V characteristics of polyacrylamide (c) Time-dependent photoresponse of MoS_2 nanoflakes (d) I-V characteristics of MoS_2 nanoflakes (e) Time-dependent photoresponse of MoS_2-polyacrylamide (f) I-V characteristics of MoS_2-polyacrylamide.

Chapter 3 deals with the photoconduction and photodetection mechanism of the WS_2 embedded in the polyvinyl alcohol matrix. Exfoliated nanosheets of WS_2 were embedded in polyvinyl alcohol (PVOH) matrix by the solution method. The SEM micrographs show a clear indication of the incorporation of WS_2 nanosheets in the PVOH matrix. Because of their intrinsic flexibility, solution processability, large-area preparation, and designable molecular structure, polymer materials are prospective materials for a new generation of photodetectors. Different molecular design approaches and innovative device designs are used to achieve it [30]. To achieve high detectivity in all-polymer photodetectors (all-PPDs), thick-film photoactive layers are chosen since they can effectively lower the dark current density. The responsivity of the device is decreased by increased recombination loss, which occurs when the photoactive layer is excessively thick [31, 32]. Because the exciton binding energy of organic semiconductor materials is approximately 0.1-1.4 eV, which is three orders higher than that of inorganic semiconductor materials, so that impact ionization cannot occur in organic photodetectors such as found in inorganic avalanche photodiodes [31] and trap-assisted carrier tunnelling effects have been primarily responsible for helping to identify the working mechanism of organic photodetectors [33]. XRD results show the hexagonal-type crystal structure of WS_2 nanosheets with the space group of P63/mmc. Tauc plot of the UV-Visible absorption spectrum of WS_2 PVOH matrix shows the optical band gap energy of 3.51 eV which is intermediated between the WS_2 nanosheets and PVOH matrix. Zeta potential of the WS_2 nanosheets, PVOH and WS_2 PVOH were found to be -10.60 mV, -4.**14** mV and -1.12 mV. Electrical measurements suggest the hopping mechanism of the charge conduction and the photoelectrical response of the materials are shown in Fig. 3. Response and detectivity were determined to be 369.130 mA/W and 5.25×1011 Jones, respectively, in the photoconduction measurement.

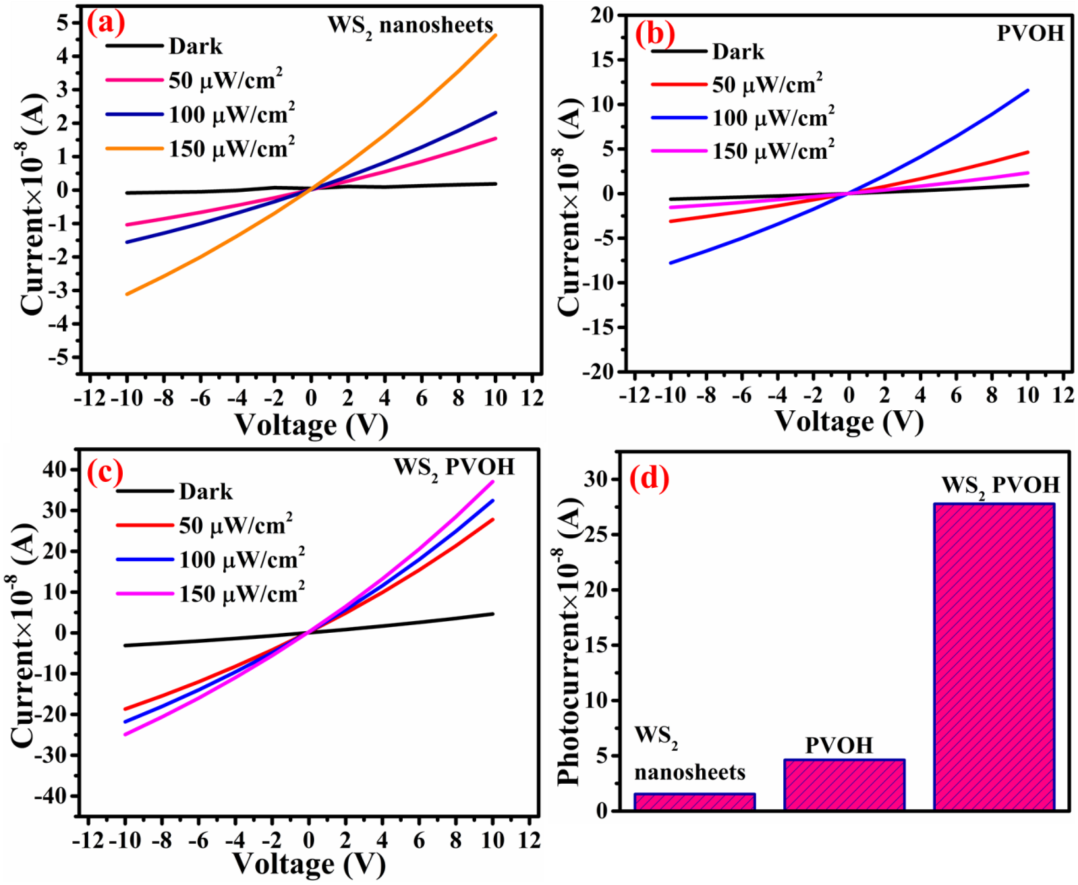

Fig. 3. Current-voltage characteristics of (a) WS$_2$ nanosheets (b) PVOH (c) WS$_2$ PVOH (d) Comparison in photocurrent in WS$_2$, PVOH and WS$_2$ PVOH at 10 V under illumination intensity of 50 μW/cm^2.

Chapter 4 deals with the two-dimensional WS$_2$-polyacrylamide metal-organic frameworks (MOFs) which are prepared via an energy-efficient solvent-free frontal polymerization method and further used as a biocompatible, flexible and low threshold high-performance photoconduction. The real images of the frontal polymerization are presented in Fig. 4. In the current study, a biocompatible, flexible, and low-threshold metal-organic framework (MOF) for high-performance photodetection was created using two-dimensional WS$_2$-polyacrylamide nanocomposites that were created using the solvent-free frontal polymerization process. Compared to other conventional methods, frontal polymerization has various advantages, including low energy consumption, no waste production, and a slower reaction time. After delivering the first input of heat, no additional heat is needed for the reaction because of its selfpropagating nature. For fabricating biocompatible and flexible photoconversion devices, these MOFs are coated on the normal paper substrate and carbon nanotubes are used as the electrodes. Scanning and Tunnelling electron microscopic (SEM and TEM) images exhibit the nanosheets-like structure and clear incorporation of WS_2 nanosheets in polyacrylamide matrix. X-ray photoelectron spectroscopy (XPS) analysis shows the peaks of W $5p_{3/2}$, W $4f_{3/2}$ and W $4f_{7/2}$ at the binding energies of 38.48, 34.98 and 32.88 eV confirms the presence of W with a valance of +4. Further investigations on MOFs were carried out by UV- Visible spectroscopy, Raman spectroscopy, Fourier transform infrared spectroscopy (FTIR), Dynamic light scattering (DLS) and Differential scanning calorimetric (DSC) analysis. This environmentally acceptable device shows the very appreciable responsivity and detectivity of 1.37 AW^{-1} and 1.52×10^{12} Jones respectively. The highest external quantum efficiency (EQE) and linear dynamic range (LDR) were found to be 465.93 % and 28.67 dB respectively with the noise equivalent power (NEP) of 3.68×10^{-8} W.

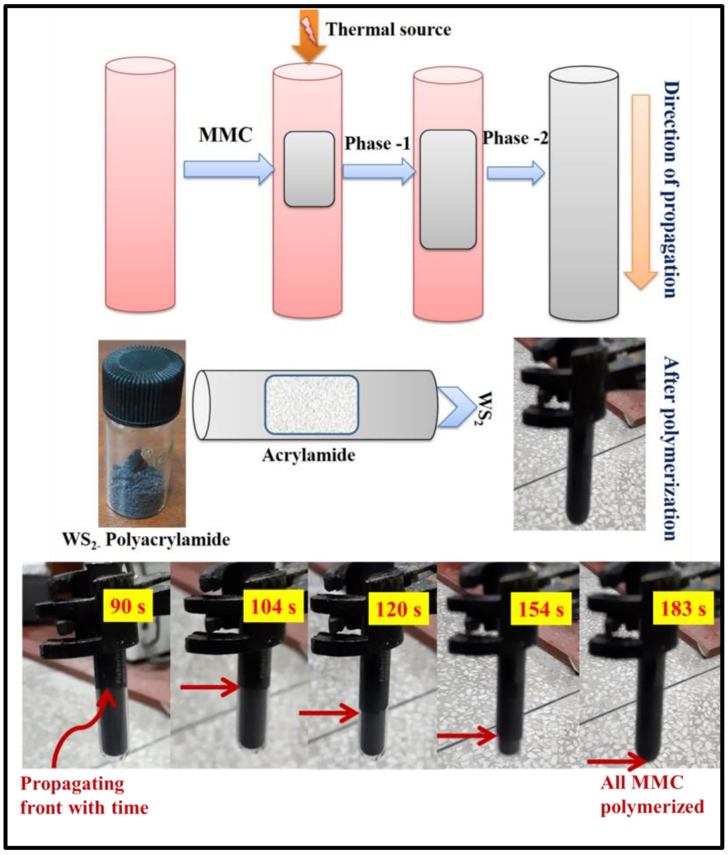

Fig. 4. A synthesis procedure for the preparation of MOFs by frontal polymerization.

Chapter 5 demonstrates the paper electronics-based device of the Bi_2S_3 nanorods (NRs) incorporated in chemically oxidized p-TSA conjugated polyaniline matrix for a high external quantum efficient device. These Bi_2S_3 NRs incorporated in the polyaniline matrix for making interconnected micro-level p-n junctions between these materials. It is generally known that a photomultiplication mechanism can considerably boost the photocurrent, producing high EQE and detectivity but requiring complicated device processing technologies. Hiramoto et al. used the photomultiplication phenomena to report an extraordinarily high EQE of 10000%. Guo et al. [34] reported the nanocomposite of ultraviolet based on interfacial trap-controlled charge injection by ZnO nanoparticles doped into P3HT:PC61BM. The highest EQEs reached up to 245300% and 340600% for the PVK:ZnO and P3HT:ZnO devices respectively [35]. The major goal of this study is to achieve photomultiplication for high EQE in the polyaniline matrix incorporated with Bi_2S_3 NRs at very low applied bias potential. The role of the Bi_2S_3-polyaniline and Ag electrodes at the interface as well as the interaction between the Bi_2S_3 NRs and polyaniline matrix has both been thoroughly investigated. The flexible, biodegradable cellulose paper was used to create the device. According to XPS data, the levels Bi $4f_{7/2}$ and Bi $4f_{5/2}$, which were discovered with binding energies of 156.88 eV and 161.98 eV, respectively, correlate to the doublet splitting of Bi. UV-Visible exhibited the optical band gap of Bi_2S_3-polyaniline found to be 2.64 eV. The metal-semiconductor-metal (MSM) device is fabricated on cellulose paper, which gave flexibility to the device structure. The light-to-photocurrent conversion capability of the device is presented in Fig. 5. This metallopolymeric energy device shows a large photoresponsivity of 16.85 A/W with sufficiently high external quantum efficiency (EQE) of 3.93×103% at extremely low drift potential of 0.1 V and extremely small optical power of 50 $\mu W/cm^2$. Additionally, the device exhibits notable responsiveness when flexible without the use of a binder. Capacitance measurements with frequency and trap depth energy measurements with trap density were also carried out to better substantiate the photoconduction phenomenon.

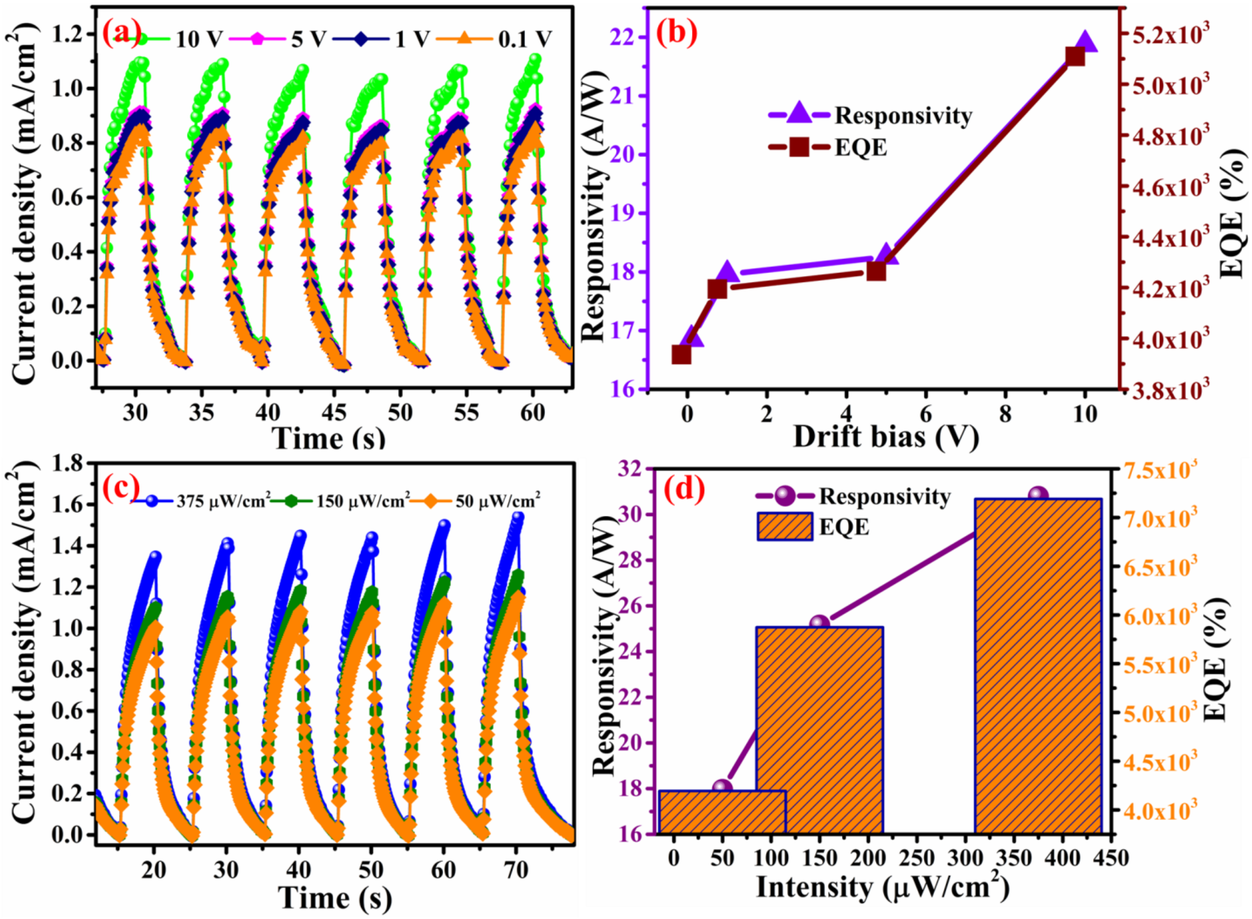

Fig. 5. (a) Transient photodetection measurement at different bias potentials (b) Responsivity and detectivity at different drift potentials (c) Transient photodetection measurement at different light intensities (d) Responsivity and detectivity at different light intensities.

Chapter 6 reports the functionalization of p-TSA (poly-toluenesulfonic acid) doped polyaniline matrix by ZnS nanosheets. Paper and cotton are the most suitable candidates among the several substrate types for flexible device technology because of their flexibility, affordability, and environmental friendliness [36]. According to prior research, paper-based devices are the most suitable photoconductors out of all the others due to their simple construction method [37]. When transition metals are added to polymers, they can change the system between states of comparatively high and low conductivity because, unlike carbon, they can quickly change their coordination number or oxidation state. This kind of reaction makes metallopolymers suitable for both sensors and switches [8, 38]. The self-powered/nearly self-powered devices are typically designed in the form of p-n junctions, Schottky junctions, and organic-inorganic metallopolymers, due to the built-in potential electron-hole pair being quickly separated. This makes the devices operated at very low voltages different from the traditional devices [39]. The structural analysis has been performed by X-ray diffraction (XRD) studies and X-ray photoelectron spectroscopy (XPS). The Rietveld refinement confirms the cubic phase of ZnS as well as the binding energies of Zn $2p_{1/2}$ and Zn $2p_{3/2}$ at 1045.85 and 1022.83 eV respectively, confirming the Zn^{2+} state. The scanning electron microscopy (SEM) of the ZnS-polyaniline exhibits different-size mist-like morphology on both paper and cotton substrates. The tunnelling electron microscopy images revealed the ZnS nanosheets with an interplanar spacing of 0.31 nm incorporated in the polyaniline matrix. Further analysis was carried out through UV-Visible spectroscopy, Fourier transform infrared (FTIR) spectroscopy, Raman spectroscopy and Dynamic light scattering. The metal-metallopolymer nanohybrid-metal device of this metal-polymer framework is fabricated on flexible and eco-friendly cellulose paper and cotton substrates. Ohmic as well as space charge limited behaviour of current is responsible for the current-voltage characteristics. The photocurrent conversion properties as well as current-voltage characteristics are presented in Fig. 6. This flexible device exhibited the ultrahigh photoresponsivity of 396.47 AW^{-1} and giant external quantum efficiency (EQE) of 1.344×10^{5} %. Paper and cotton substrate-based devices show significant Responsivities of 3.67 and 1.74 mA/W with the detectivity of 3.09×10^{10} and 3.47×10^{10} Jones even at 0 V.

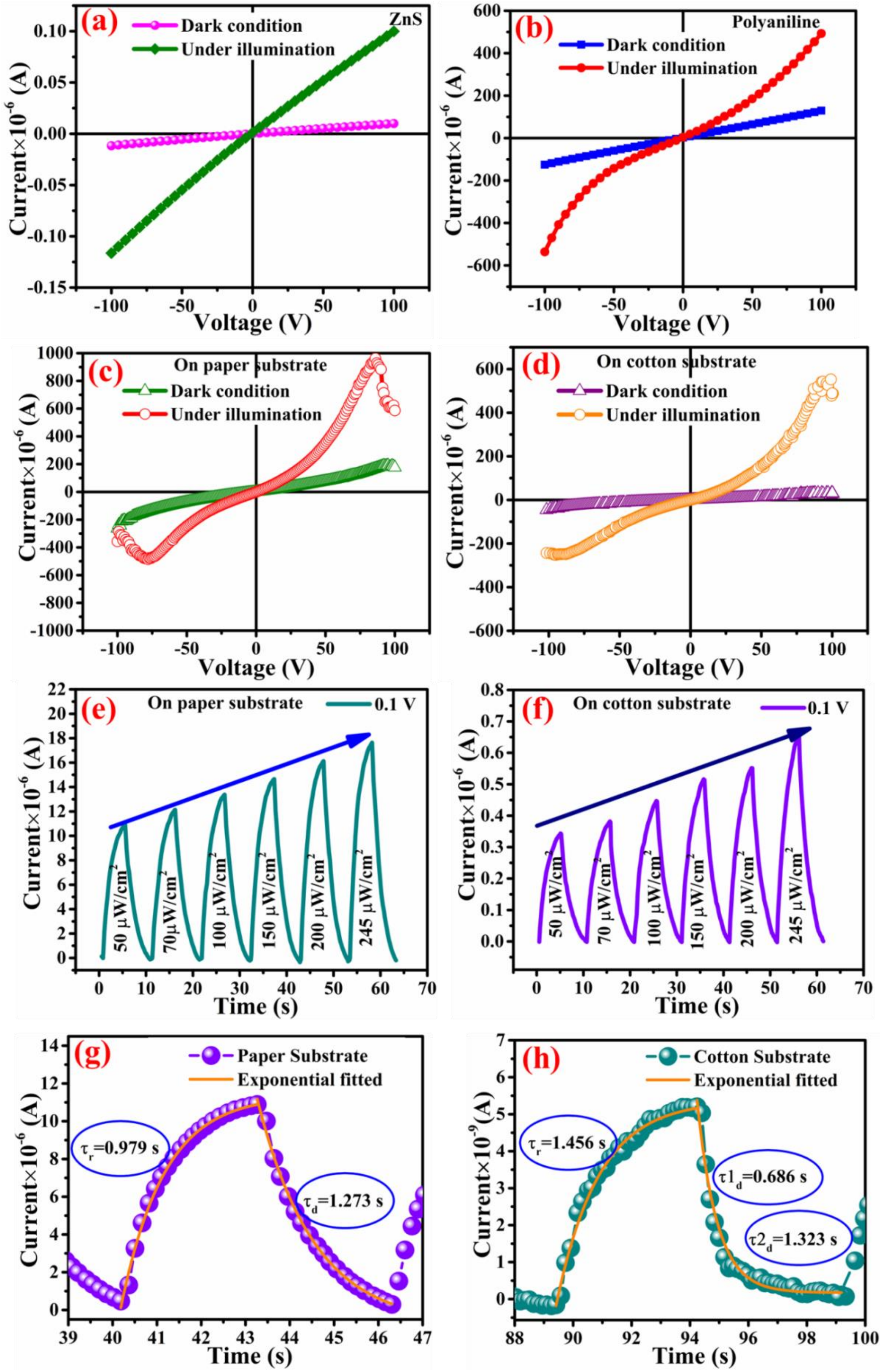
(a)
Dark condition
Under illumination
ZnS
Current×10^-6 (A)
0.10
0.05
0.00
-0.05
-0.10
-0.15
-100
-50
0
50
100
Voltage (V)
(b)
Polyaniline
Dark condition
Under illumination
Current×10^-6 (A)
600
400
200
0
-200
-400
-600
-100
-50
0
50
100
Voltage (V)
(c)
On paper substrate
Dark condition
Under illumination
Current×10^-6 (A)
1000
800
600
400
200
0
-200
-400
-600
-800
-1000
-100
-50
0
50
100
Voltage (V)
(d)
On cotton substrate
Dark condition
Under illumination
Current×10^-6 (A)
600
400
200
0
-200
-400
-600
-100
-50
0
50
100
Voltage (V)
(e)
On paper substrate
0.1 V
Current×10^-6 (A)
22
20
18
16
14
12
10
8
6
4
2
0
50 μW/cm²
70μW/cm²
100 μW/cm²
150 μW/cm²
200 μW/cm²
245 μW/cm²
0
10
20
30
40
50
60
70
Time (s)
(f)
On cotton substrate
0.1 V
Current×10^-6 (A)
0.8
0.7
0.6
0.5
0.4
0.3
0.2
0.1
0.0
50 μW/cm²
70 μW/cm²
100 μW/cm²
150 μW/cm²
200 μW/cm²
245 μW/cm²
0
10
20
30
40
50
60
70
Time (s)
(g)
Paper Substrate
Exponential fitted
τr=0.979 s
τd=1.273 s
Current×10^-6 (A)
14
12
10
8
6
4
2
0
39
40
41
42
43
44
45
46
47
Time (s)
(h)
Cotton Substrate
Exponential fitted
τr=1.456 s
τ1d=0.686 s
τ2d=1.323 s
Current×10^-9 (A)
7
6
5
4
3
2
1
0
88
90
92
94
96
98
100
Time (s)

Fig. 6. (a) Current-Voltage (I-V) characteristics of ZnS (b) Current-Voltage (I-V) characteristics of polyaniline (c) Current-Voltage (I-V) characteristics on paper substrate (d) Current-Voltage (I-V) characteristics on cotton substrate (e) Current power measurements for paper substrate (f) Current power measurements for cotton substrate (g) Experimental and exponentially fitted rise and decay time constants for paper substrate (h) Experimental and exponentially fitted rise and decay time constants for cotton substrate.

Table 7.1 Chapter wise outline of the Thesis

Ch.	Materials	Pin/V (μW/cm^2/ Volt)	Photo current (A)	Dark current (A)	Responsivity (A/W)	External quantum efficiency (%)	Detectivity (Jones)	Noise equivalent power (W)
1.	Introduction							
2.	MoS_2-polyacrylamide	40/5	1.46×10^{-7}	2.74×10^{-9}	0.060	20.37	4.96×10^{11}	4.57×10^{-8}
3.	WS_2-polyvinyl alcohol	50/10	7.99×10^{-7}	6.16×10^{-8}	0.36	125	5.25×10^{11}	1.67×10^{-7}
4.	WS_2-polyacrylamide	50/5	1.37×10^{-6}	5.06×10^{-8}	1.37	465.93	1.52×10^{12}	3.68×10^{-8}
5.	Bi_2S_3-polyaniline	50/0.1	8.43×10^{-4}	1.00×10^{-4}	16.85	3.936×10^{3}	2.97×10^{12}	5.93×10^{-6}
6.	ZnS-polyaniline	50/86	9.61×10^{-4}	1.68×10^{-4}	396.47	1.344×10^{5}	1.07×10^{13}	4.25×10^{-7}
7.	Conclusion							

Scope of further research

- Metallopolymers have demonstrated a great potential as materials for use in battery, fuel cell, and solar cell technologies for renewable energy sources. These were found appropriate for many kinds of devices because of their distinctive electrical and optical characteristics.
- As metallopolymers may create powerful chemical connections with other substances, which can improve their performance in certain applications.
- The creation of more effective solar cells is one potential use for metallopolymers in renewable energy. Electronic and optical characteristics of these materials can be adjusted to improve the solar cell's performance and efficiency. The use of metallopolymers as catalysts in fuel cells have a very good scope for a different area of study.
- Overall, there is a lot of promise for metallopolymers to be used in renewable energy, and work is being done to investigate and create new uses for these materials. Metallopolymers offer the potential for usage in various renewable energy technologies, such as thermoelectric generators, which turn heat into electricity. Performance and efficiency of these generators can be improved by making use of their special electronic features.
- Future applications for metallopolymers can include catalysts, sensors, drug delivery systems, and water filtering. A variety of applications benefit greatly from metallopolymers because of their unique properties. Because their potential has not yet been fully realized, metallopolymers present numerous exciting options for future research and development.
- By changing the structure of the metallopolymer, the ability to adjust the composition of the metal and polymer components may enable the development of new and improved materials.

References

[1] Y. Wang, D. Astruc, A.S. Abd-El-Aziz, Metallopolymers for advanced sustainable applications, Chemical Society Reviews 48(2) (2019) 558-636.

[2] M.A. de Valle, B. González, C. Espinosa-Bustos, A.M.R. Ramírez, M. Gacitúa, L.A. Hernández, dsDNA Sensing Capabilities of Metallopolymers Electrochemically Deposited from Ruthenium-Pyrrole and-Thiophene Complexes, International Journal of Electrochemical Science 14 (2019) 8131-8140.

[3] S. Singla, N.P. Shetti, S. Basu, K. Mondal, T.M. Aminabhavi, Hydrogen production technologies-membrane based separation, storage and challenges, Journal of Environmental Management 302 (2022) 113963.

[4] A.D. Pomogailo, V.N. Kestelʹman, Metallopolymer nanocomposites, Springer Science & Business Media2006.

[5] M.T. Nguyen, R.A. Jones, B.J. Holliday, Recent advances in the functional applications of conducting metallopolymers, Coordination Chemistry Reviews 377 (2018) 237-258.

[6] R. Koutavarapu, C.V. Reddy, K. Syed, K.R. Reddy, N.P. Shetti, T.M. Aminabhavi, J. Shim, Ultra-small zinc oxide nanosheets anchored onto sodium bismuth sulfide nanoribbons as solar-driven photocatalysts for removal of toxic pollutants and phtotoelectrocatalytic water oxidation, Chemosphere 267 (2021) 128559.

[7] J. Xiang, C.-L. Ho, W.-Y. Wong, Metallopolymers for energy production, storage and conservation, Polymer Chemistry 6(39) (2015) 6905-6930.

[8] J.-C. Eloi, L. Chabanne, G.R. Whittell, I. Manners, Metallopolymers with emerging applications, Materials Today 11(4) (2008) 28-36.

[9] S. Singla, S. Sharma, S. Basu, N.P. Shetti, T.M. Aminabhavi, Photocatalytic water splitting hydrogen production via environmental benign carbon based nanomaterials, International Journal of Hydrogen Energy 46(68) (2021) 33696-33717.

[10] M. Gallei, C. Rüttiger, Recent trends in metallopolymer design: redox-controlled surfaces, porous membranes, and switchable optical materials using ferrocene-containing polymers, Chemistry–A European Journal 24(40) (2018) 10006-10021.

[11] M. Szuwarzyński, K. Wolski, T. Kruk, S. Zapotoczny, Macromolecular strategies for transporting electrons and excitation energy in ordered polymer layers, Progress in Polymer Science 121 (2021) 101433.

[12] D.C. Olson, Y.-J. Lee, M.S. White, N. Kopidakis, S.E. Shaheen, D.S. Ginley, J.A. Voigt, J.W.P. Hsu, Effect of polymer processing on the performance of poly (3-hexylthiophene)/ZnO nanorod photovoltaic devices, The Journal of Physical Chemistry C 111(44) (2007) 16640-16645.

[13] N.C. Das, S. Biswas, P.E. Sokol, The photovoltaic performance of ZnO nanorods in bulk heterojunction solar cells, Journal of Renewable and Sustainable Energy 3(3) (2011) 033105.

[14] N.C. Das, P.E. Sokol, Hybrid photovoltaic devices from regioregular polythiophene and ZnO nanoparticles composites, Renewable Energy 35(12) (2010) 2683-2688.

[15] M. Helgesen, R. Søndergaard, F.C. Krebs, Advanced materials and processes for polymer solar cell devices, Journal of Materials Chemistry 20(1) (2010) 36-60.

[16] Y. Xie, P. Joshi, S.B. Darling, Q. Chen, T. Zhang, D. Galipeau, Q. Qiao, Electrolyte effects on electron transport and recombination at ZnO nanorods for dye-sensitized solar cells, The Journal of Physical Chemistry C 114(41) (2010) 17880-17888.

[17] G.D. Sharma, A. Agrawal, A.C. Schlachter, G. Marineau-Plante, P.D. Harvey, Efficient ternary bulk heterojunction organic solar cells using a low-cost nonfullerene acceptor, Journal of Materials Chemistry C (2022).

[18] C.V. Reddy, K.R. Reddy, N.P. Shetti, J. Shim, T.M. Aminabhavi, D.D. Dionysiou, Hetero-nanostructured metal oxide-based hybrid photocatalysts for enhanced photoelectrochemical water splitting–a review, International journal of hydrogen energy 45(36) (2020) 18331-18347.

[19] K. Gurunathan, A.V. Murugan, R. Marimuthu, U.P. Mulik, D.P. Amalnerkar, Electrochemically synthesised conducting polymeric materials for applications towards technology in electronics, optoelectronics and energy storage devices, Materials Chemistry and Physics 61(3) (1999) 173-191.

[20] S. Singh, P. Yadav, M.K. Gupta, G.I. Dzhardimalieva, J. Yoon, C. Maiti, B.C. Yadav, Gigantic stimulation in response by solar irradiation in self-healable and self-powered LPG sensor based on triboelectric nanogenerator: Experimental and DFT computational study, Sensors and Actuators B: Chemical 359 (2022) 131573.

[21] G.R. Whittell, I. Manners, Metallopolymers: new multifunctional materials, Advanced Materials 19(21) (2007) 3439-3468.

[22] S. Goetz, S. Zechel, M.D. Hager, G.R. Newkome, U.S. Schubert, Versatile applications of metallopolymers, Progress in Polymer Science 119 (2021) 101428.

[23] C.-L. Ho, W.-Y. Wong, Metal-containing polymers: Facile tuning of photophysical traits and emerging applications in organic electronics and photonics, Coordination Chemistry Reviews 255(21-22) (2011) 2469-2502.

[24] T. Katsume, M. Hiramoto, M. Yokoyama, Photocurrent multiplication in naphthalene tetracarboxylic anhydride film at room temperature, Applied Physics Letters 69(24) (1996) 3722-3724.

[25] G.R. Whittell, M.D. Hager, U.S. Schubert, I. Manners, Functional soft materials from metallopolymers and metallosupramolecular polymers, Nature Materials 10(3) (2011) 176-188.

[26] C.J. Brabec, S. Gowrisanker, J.J.M. Halls, D. Laird, S. Jia, S.P. Williams, Polymer–fullerene bulk-heterojunction solar cells, Advanced Materials 22(34) (2010) 3839-3856.

[27] C. Zhou, W.-x. Zhao, F.-t. You, Z.-x. Geng, H.-s. Peng, Highly stable and luminescent oxygen nanosensor based on ruthenium-containing metallopolymer for real-time imaging of intracellular oxygenation, ACS sensors 4(4) (2019) 984-991.

[28] B.J. Holliday, T.M. Swager, Conducting metallopolymers: the roles of molecular architecture and redox matching, Chemical Communications (1) (2005) 23-36.

[29] Y.-J. Cheng, S.-H. Yang, C.-S. Hsu, Synthesis of conjugated polymers for organic solar cell applications, Chemical Reviews 109(11) (2009) 5868-5923.

[30] D. Zhu, D. Ji, L. Li, W. Hu, Recent progress in polymer-based infrared photodetectors, Journal of Materials Chemistry C 10 (2022) 13312-13323.

[31] L. Shi, Q. Liang, W. Wang, Y. Zhang, G. Li, T. Ji, Y. Hao, Y. Cui, Research progress in organic photomultiplication photodetectors, Nanomaterials 8(9) (2018) 713.

[32] Z. Zhong, K. Li, J. Zhang, L. Ying, R. Xie, G. Yu, F. Huang, Y. Cao, High-performance all-polymer photodetectors via a thick photoactive layer strategy, ACS Applied Materials and Interfaces 11(15) (2019) 14208-14214.

[33] M. Ahmadi, T. Wu, B. Hu, A review on organic–inorganic halide perovskite photodetectors: device engineering and fundamental physics, Advanced Materials 29(41) (2017) 1605242.

[34] M. Hiramoto, T. Imahigashi, M. Yokoyama, Photocurrent multiplication in organic pigment films, Applied Physics Letters 64(2) (1994) 187-189.

[35] I.H. Campbell, B.K. Crone, Bulk photoconductive gain in poly (phenylene vinylene) based diodes, Journal of Applied Physics 101(2) (2007) 024502.

[36] A.T. Vicente, A. Araújo, M.J. Mendes, D. Nunes, M.J. Oliveira, O. Sanchez-Sobrado, M.P. Ferreira, H. Águas, E. Fortunato, R. Martins, Multifunctional cellulose-paper for light harvesting and smart sensing applications, Journal of Materials Chemistry C 6(13) (2018) 3143-3181.

[37] D. Kaur, M. Kumar, A Strategic Review on Gallium Oxide Based Deep-Ultraviolet Photodetectors: Recent Progress and Future Prospects, Advanced Optical Materials (2021) 2002160.

[38] K.L. Bhowmik, K. Deb, A. Bera, R.K. Nath, B. Saha, Charge transport through polyaniline incorporated electrically conducting functional paper, The Journal of Physical Chemistry C 120(11) (2016) 5855-5860.

[39] B.D. Boruah, Zinc oxide ultraviolet photodetectors: rapid progress from conventional to self-powered photodetectors, Nanoscale Advances 1(6) (2019) 2059-2085.

LIST OF PUBLICATIONS

Part of the thesis published in the refereed journals:

1. **A. Verma,** P. Chaudhary, R.K. Tripathi, A. Singh, B.C. Yadav, State of the art metallopolymer based functional nanomaterial for photodetector and solar cell application, Journal of Inorganic and Organometallic Polymers and Materials 32(8) (2022) 2807-2826.

2. **A. Verma,** P. Chaudhary, R.K. Tripathi, B.C. Yadav, The functionalization of polyacrylamide with MoS2 nanoflakes for use in transient photodetectors, Sustainable Energy and Fuels 5(5) (2021) 1394-1405.

3. **A. Verma,** A. Singh, P. Chaudhary, R.K. Tripathi, B.C. Yadav, P. Chauhan, D. Kumar, Photocurrent conversion capability of a 2D WS_2-polyvinyl alcohol matrix and its DFT-based charge carrier dynamics analysis, Materials Advances 4(4) (2023) 1062-1074.

4. **A. Verma,** P. Chaudhary, R.K. Tripathi, B.C. Yadav, Flexible, environmentally-acceptable and long-durable-energy-efficient novel WS_2–polyacrylamide MOFs for high-performance photodetectors, Materials Advances 3 (2022) 3994-4005.

5. **A. Verma,** P. Chaudhary, A. Singh, R.K. Tripathi, B.C. Yadav, ZnS nanosheets in a polyaniline matrix as metallopolymer nanohybrids for flexible and biofriendly photodetectors, ACS Applied Nano Materials 5(4) (2022) 4860-4874.

6. **A. Verma,** P. Chaudhary, A. Singh, R. K. Tripathi, B. C. Yadav, P. Chauhan, Photomultiplicative and high external quantum efficient energy conversion device for paper electronics, ACS Applied Electronic Materials (Under review) (Manuscript ID: el-2023-006733)

Work not included in Thesis

1. R.K. Tripathi, O.S. Panwar, I. Rawal, C.K. Dixit, **A. Verma,** P. Chaudhary, A.K. Srivastava, B.C. Yadav, Study of variable range hopping conduction mechanism in nanocrystalline carbon thin films deposited by modified anodic jet carbon arc technique: application to light-dependent resistors, Journal of Materials Science: Materials in Electronics 32 (2021) 2535-2546.

2. **A. Verma,** P. Chaudhary, R.K. Tripathi, B.C. Yadav, Transient photodetection studies on 2D ZnO nanostructures prepared by simple organic-solvent assisted route, Sensors and Actuators A: Physical 321 (2021) 112600.

3. A. Singh, S. Sikarwar, **A. Verma,** B.C. Yadav, The recent development of metal oxide heterostructures based gas sensor, their future opportunities and challenges: a review, Sensors and Actuators A: Physical 332 (2021) 113127.

4. P. Chaudhary, D.K. Maurya, A. Pandey, **A. Verma,** R.K. Tripathi, S. Kumar, B.C. Yadav, Design and development of flexible humidity sensor for baby diaper alarm: Experimental and theoretical study, Sensors and Actuators B: Chemical 350 (2022) 130818.

5. C. Gautam, **A. Verma,** P. Chaudhary, B.C. Yadav, Development of 2D based ZnO–MoS_2 nanocomposite for photodetector with light-induced current study, Optical Materials 123 (2022) 111860.

6. A. Singh, **A. Verma,** B. Yadav, P. Chauhan, Earth-abundant and environmentally benign Ni–Zn iron oxide intercalated in a polyaniline based nanohybrid as an ultrafast photodetector, Dalton Transactions 51(20) (2022) 7864-7877.

7. P. Chaudhary, **A. Verma,** A. Mishra, D. Yadav, K. Pal, B. Yadav, E.R. Kumar, K.B. Thapa, S. Mishra, D.K. Dwivedi, Preparation of carbon quantum dots using bike pollutant soot: Evaluation of structural, optical and moisture sensing properties, Physica E: Low-dimensional Systems and Nanostructures 139 (2022) 115174.

8. **A. Verma,** U. Kumar, P. Chaudhary, B.C. Yadav, Investigation on structural and optical properties of porous SnO_2 nanomaterial fabricated by direct liquid injection chemical vapour deposition technique, Solid State Communications 348 (2022) 114723.

9. **A. Verma,** D. Yadav, A. Singh, M. Gupta, K.B. Thapa, B.C. Yadav, Detection of acetone via exhaling human breath for regular monitoring of diabetes by low-cost sensing device based on perovskite $BaSnO_3$ nanorods, Sensors and Actuators B: Chemical 361 (2022) 131708.

10. R. Raj, P. Lohia, D.K. Dwivedi, **A. Verma,** B.C. Yadav, High-responsivity $(Ga_2Ge)_{100-x}(Ga_3Sb_2)_x$ (x= 15, 30, 45, 60) photodetection sensor for optoelectronic applications, Journal of Materials Science: Materials in Electronics 33(22) (2022) 17939-17948.

11. A. Singh, **A. Verma,** B.C. Yadav, MnO_2-SnO_2 based liquefied petroleum gas sensing device for lowest explosion limit gas concentration, ECS Sensors Plus 1(2) (2022) 025201.

12. M. Gupta, P. Chaudhary, A. Singh, **A. Verma,** D. Yadav, B.C. Yadav, Development of MoO_3-CdO nanoparticles based sensing device for the detection of harmful acetone levels in our skin and body via nail paint remover, Sensors and Actuators B: Chemical 368 (2022) 132102.

13. S. Sharma, **A. Verma,** P. Chaudhary, A. Singh, R.K. Tripathi, M. Gupta, B.C. Yadav, Structural and photodetection studies of hydrothermally grown anatase TiO_2 nanomaterial, Materials Today: Proceedings 73 (2023) 255-262.

14. A. Kumar, **A. Verma,** A. Singh, B.C. Yadav, Wet chemical preparation of CdS nanoparticles for the photodetection application, Materials Today: Proceedings 73 (2023) 337-341.

15. A. Singh, P. Chauhan, **A. Verma,** B.C. Yadav, $CuBi_2O_4$ nanocrystals integrated with polyaniline nanobelt arrays for weak light photomultiplication type photodetector, Sustainable Energy and Fuels (2023).

16. A. Singh, S.K. Yadav, **A. Verma,** S. Sikarwar, B.C. Yadav, Hydrothermally Synthesized $ZnSnO_3$ Nanoflakes Based Low-Cost Sensing Device for High Performance CO_2 Monitoring, ECS Advances 2(1) (2023) 016501.

17. A. Sharma, P. Chaudhary, **A. Verma,** R.K. Tripathi, R. Kumar, G. Gupta, D.P. Mondal, B.C. Yadav, A.K. Srivastava, Novel 3D lightweight carbon foam for ultrasensitive humidity sensor operated at different frequencies, ECS Journal of Solid State Science and Technology 12(2) (2023) 027004.

18. R. Raj, P. Lohia, D. Dwivedi, P.K. Singh, **A. Verma,** B.C. Yadav, High-performance photodetection sensors based on $(S_2Ge)_{100-x}(S_3Sb_2)_x$ (x= 15, 30, 45, 60) system for optoelectronics applications, Journal of Materials Science: Materials in Electronics 34(11) (2023) 948.

19. **A. Verma,** B.C. Yadav, 2D/2D Nanostructured System Based on WO_3/WS_2 for Acetone Sensor and Breath Analyzer, ACS Applied Nano Materials 6(7) (2023) 5493-5507.

20. A. Singh, A. Singh, **A. Verma,** B.C. Yadav, V. Chaudhary, Economic $ZnCo_2O_4$ Nanoflakes Chemiresistor Assisted Room-Temperature Monitoring of Low Trace Airborne Ammonia, ECS Journal of Solid State Science and Technology 12(4) (2023) 047005.

21. M. Mathur, **A. Verma,** A. Singh, B.C. Yadav, V. Chaudhary, $CuMoO_4$ nanorods-based acetone chemiresistor-enabled non-invasive breathomic-diagnosis of human diabetes and environmental monitoring, Environmental Research 229 (2023) 115931.

22. P. Yadav, K. Sahay, **A. Verma,** D.K. Maurya, B.C. Yadav, Applications of multifunctional triboelectric nanogenerator (TENG) devices: materials and prospects, Sustainable Energy & Fuels, 7 (2023) 3796-3831.

23. A. Singh, P. Chauhan, **A. Verma,** B.C. Yadav, An investigation into the hybrid architecture of Mn–Co nanoferrites incorporated into a polyaniline matrix for photoresponse studies, Physical Chemistry Chemical Physics (2023).

Papers presented in International Conferences/Proceedings

1. Poster presentation in "National conference on Advanced Nanomaterials and their Application (ANA-2018)", organized by department of Physics at Motilal Nehru National Institute of Technology (MNNIT-Allahabad), held on 21-23 December, 2018, Prayagraj, India

2. Oral presentation in " International Webinar on Nanoscience and Nanotechnology (IWNN-2020)" on 27th to 29th November, 2020, Organized by Department of Physics, School of Physical and Decision Sciences, Babasaheb Bhimrao Ambedkar University (A Central University), Lucknow, India.

3. Oral presentation in "National Conference on Innovation and Technology for Sustainable Rural Development" on 1-2, July, 2022 at Babasaheb Bhimrao Ambedkar University, Lucknow, U.P., India

4. Oral presentation in "International Conference on Advances in Materials for Health, Environment and Circular Economy (ICAMTHEC-2022)" on 25-26, November, 2022, organized by School of Applied &Life Sciences, Uttaranchal University, Dehradun, India.

5. Oral presentation in National Science day conference " Global Science for Global wellbeing" organized by Department of Physics, Babasaheb Bhimrao Ambedkar University, Lucknow (Best oral presentation award)